R42

3D near-infrared imaging based on a SPAD image sensor

Juan Mata Pavia[a,b], Cristiano Niclass[a], Claudio Favi[a], Martin Wolf[b] , Edoardo Charbon[a,c]

[a]Ecole Polytechnique Fédérale de Lausanne (EPFL), Quantum Architecture Group(AQUA), 1015 Lausanne, Switzerland
[b]University Hospital Zürich(USZ), Biomedical Optics Research Laboratory(BORL), Division of Neonatology, 8091 Zürich, Switzerland
[c]TU Delft, 2628CD Delft, Netherlands

ABSTRACT

A new imager for 3D near-infrared imaging has been designed based on a single-photon avalanche diode (SPAD) imager with 128x128 pixels capable of performing time-resolved measurements with a resolution of 97ps. The imager linearity has been improved to make more accurate measurements. A new optical setup has been implemented in order to prove the suitability of this kind of sensors for this application.

1. INTRODUCTION

Optical tomography is a technique to image human tissue such as breast or brain using light absorption as main contrast. Recently, researchers have demonstrated that it is possible to improve the image quality by using large data sets coming from CCD cameras.[1–3] Time-resolved techniques enable better depth resolution, thus improving the quality of the reconstructions.[4] In this paper, the aim is to show how recently developed single-photon avalanche diode (SPAD) imagers[5] can open new frontiers in optical tomography.

2. SETUP

The SPAD sensor works in time-correlated single-photon counting (TCSPC) mode and provides time-resolved measurements for each of its 128x128 pixels independently.[5] Figures 1 and 2 show the sensor architecture and a picture of the manufactured chip. This sensor exhibited high levels of non-linearity which were compensated by the application of dithering to the synchronization signal. However the integral non-linearity levels were still too high for our application.[5] The main problem was the multi-level interpolation architecture of the time-to-digital converter (TDC). Codes that were close to the beginning or the end of one of the levels were prone to exhibit non-linearities. In order to reduce the non-linearity, a new method was implemented where incoming photons that produced those codes were discarded. By applying dithering, the complete range was covered. Figures 3 and 4 show the original non-linearity result together with the results for the two dithering methods. With the new method the integral non-linearity is improved from almost 2LSB to 0.25LSB. Figure 5 shows the impulse response function of one of the pixels to a laser pulse.

A new illumination system has been conceived that trades off image reconstruction complexity with sensor speed. The adopted solution was to illuminate the object under study with lines outside the field of view of the camera. Thus, the light captured by the sensor undergoes several scattering events before it is detected, making its temporal point-spread function much smoother. Figure 6 shows the response at one pixel for this application. Figures 7 and 8 show the new optical setup and its implementation. For the experiments, we use as target a liquid phantom that mimics the optical properties of a human breast. Small silicon heterogeneities with higher absorption coefficient μ_a are introduced in the liquid.

Send correspondence to J. Mata Pavia, UniversitätsSpital Zürich, Klinik für Neonatologie, Frauenklinikstrasse 10, 8091 Zürich, Switzerland, E-mail: juan.matapavia@epfl.ch, Telephone: +41 (0)44 556 3032

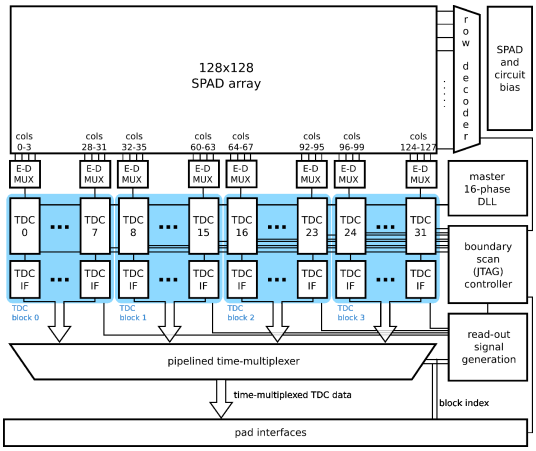

Figure 1. SPAD Image Sensor Architecture. The sensor consists of a 128x128 pixel array, a bank of 32 TDCs, and a fast parallel readout circuitry. A row decoding logic selects 128 pixels that are activated for detection. The pixels are organized in groups of four that access the same TDC based on a first-in-take-all sharing scheme.

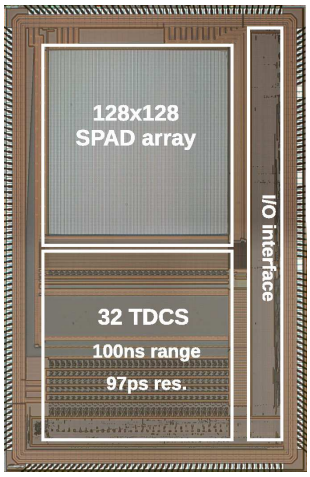

Figure 2. Micrograph of the circuit, fabricated in 0.35μm CMOS technology. It has a surface of 8x5mm2, the pixel pitch is 25μm. The TDCs have a resolution of 97ps and a 100ns range.

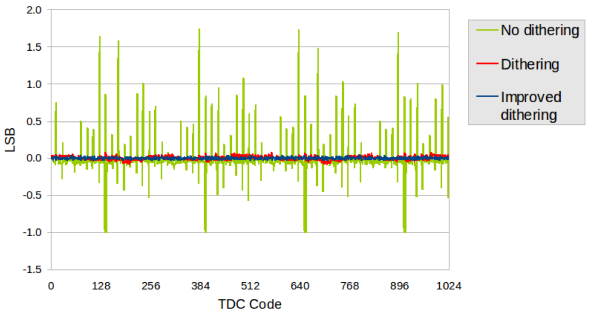

Figure 3. Differential non-linearity for the different methods.

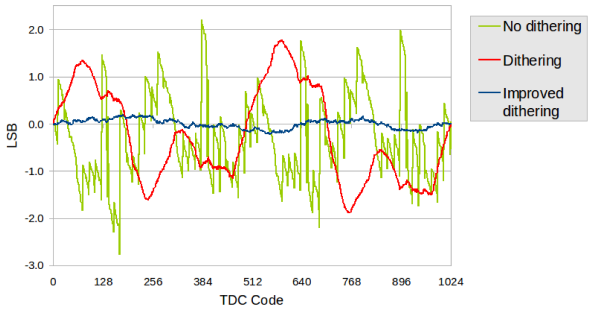

Figure 4. Integral non-linearity for the different methods.

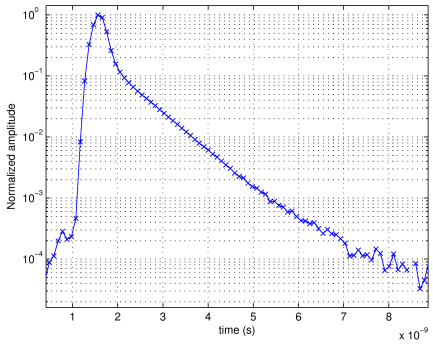

Figure 5. Impulse response function of one pixel to a pulse of light generated by a picosecond laser (Becker & Hickl, BHL-700, 780nm, 3mW) reflected by a black target.

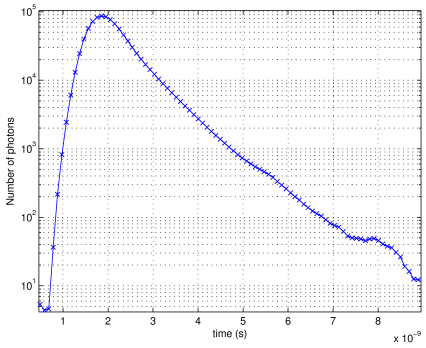

Figure 6. Typical response of one pixel for time resolved near-infrared imaging. A picosecond laser was used to illuminate a phantom with $\mu_a = 0.07cm^{-1}$ and $\mu_s' = 5cm^{-1}$. The source detector separation was 2cm.

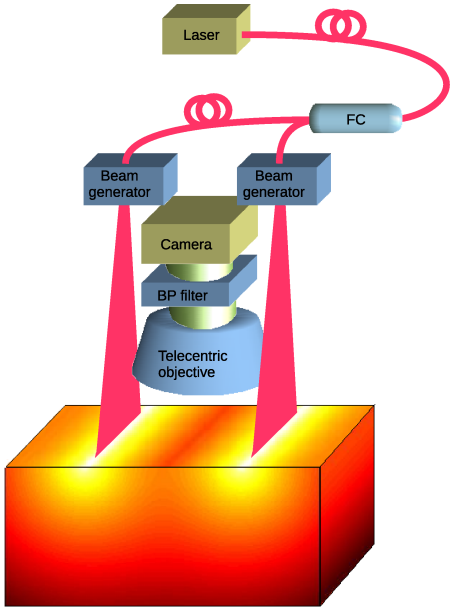

Figure 7. Diagram of the new optical setup for NIRI. A picosecond laser is used to generate lines of light on the surface of the object under study

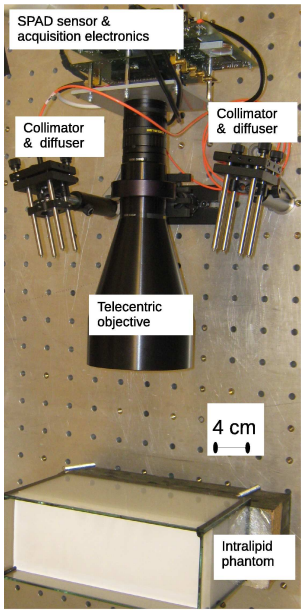

Figure 8. Setup implementation for the experiments. The lines on the surface of the phantom are generated by means of a collimator and a line diffuser. The liquid phantom is composed of distilled water, an intralipid emulsion and Indian ink.

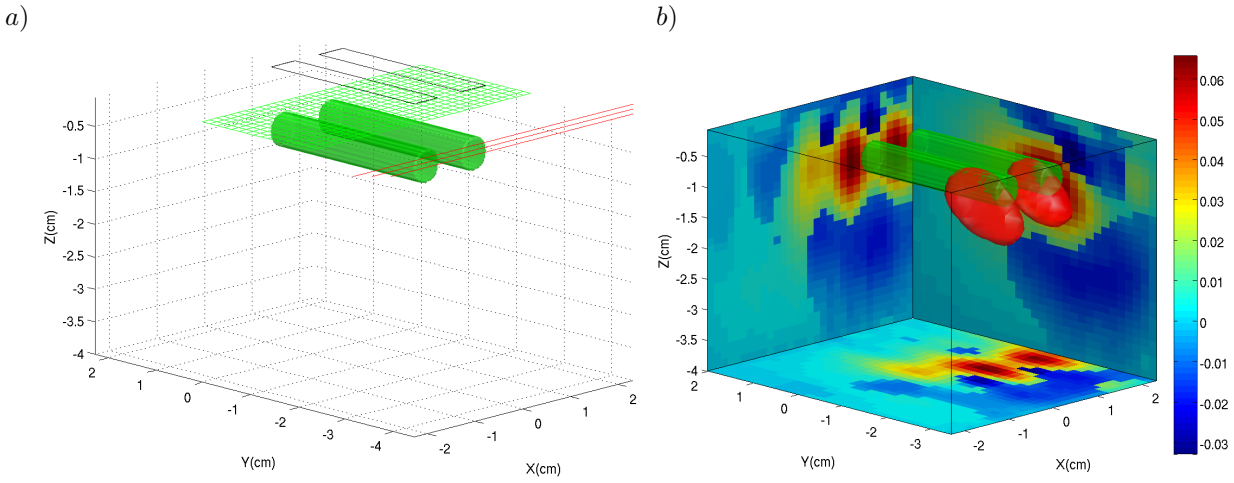

Figure 9. a) Setup used to evaluate the systems resolution. The volume represents the phantom with two 5mm diameter cylinders separated 5mm from each other. The phantom has $\mu_a = 0.07cm^{-1}$ and $\mu'_s = 5cm^{-1}$, and the embedded objects have $\mu_a = 0.25cm^{-1}$ and $\mu'_s = 5cm^{-1}$. b) Reconstruction from the experimental measurement. The green volumes represent the original objects, while the red ones are the reconstructed ones.

3. RESULTS

As described in literature,[6] the problem is ill posed by nature. For this reason, regularization is a key factor in the image reconstruction algorithm. We performed several simulations with different regularization algorithms and the best results were obtained using the sub-space preconditioned least square root (SP-LSQR) algorithm.[7] We performed several experiments with a homogeneous phantom with two embedded cylinders. Figure 9b) shows the reconstruction obtained from the measured, experimental data. We can clearly distinguish two objects embedded in the phantom. Only one section of the cylinders is detected accurately, because only one line was projected and thus the other half of the cylinders was not illuminated enough. Despite, the current limitations, our prototype demonstrates a target detection consistent with a spatial uncertainty of less than 5mm, thus showing the suitability of the approach to the target applications.

4. CONCLUSIONS

We demonstrated the suitability of SPAD imagers for 3D near-infrared imaging, providing both high spatial resolution and time-resolved measurements. We expect that new imagers with higher time resolution and more pixels will significantly improve the quality of the reconstructions.

REFERENCES

[1] Markel, V. A. and Schotland, J. C., "Inverse problem in optical diffusion tomography. I. Fourier-Laplace inversion formulas," *J. Opt. Soc. Am. A* **18**, 1336–1347 (Jun 2001).

[2] Abookasis, D., Lay, C. C., Mathews, M. S., Linskey, M. E., Frostig, R. D., and Tromberg, B. J., "Imaging cortical absorption, scattering, and hemodynamic response during ischemic stroke using spatially modulated near-infrared illumination," *J Biomed Opt* **14**, 024033 (2009).

[3] Konecky, S. D., Mazhar, A., Cuccia, D., Durkin, A. J., Schotland, J. C., and Tromberg, B. J., "Quantitative optical tomography of sub-surface heterogeneities using spatially modulated structured light," *Opt. Express* **17**, 14780–14790 (Aug 2009).

[4] Ntziachristos, V., Ripoll, J., Wang, L. V., and Weissleder, R., "Looking and listening to light: the evolution of whole-body photonic imaging," *Nat. Biotechnol.* **23**, 313–320 (Mar 2005).

[5] Niclass, C., Favi, C., Kluter, T., Gersbach, M., and Charbon, E., "A 128x128 single-photon image sensor with column-level 10-bit time-to-digital converter array," *Solid-State Circuits, IEEE Journal of* **43**(12), 2977–2989 (2008).

[6] O'Leary, M. A., *Imaging with diffuse photon density waves*, PhD thesis, University of Pennsylvania (1996).

[7] Jacobsen, M., Hansen, P., and Saunders, M., "Subspace preconditioned lsqr for discrete ill-posed problems," *BIT Numerical Mathematics* **43**, 975–989 (2003). 10.1023/B:BITN.0000014547.88978.05.